

Reduced Hamiltonian for Electronic States of Dilute Nitride Semiconductors

Masato Morifuji¹ and Fumitaro Ishikawa²

¹Graduate School of Engineering, Osaka University, 2-1 Yamada-oka, Suita, Osaka 565-0871, Japan

²Graduate School of Science and Engineering, Ehime University, 3 Bunkyo-cho, Matsuyama, Ehime 790-8577, Japan

(Dated: October 16, 2018)

We present a novel model to describe conduction band of $\text{GaN}_x\text{As}_{1-x}$ (GaNAs). As well known, GaNAs shows exotic behavior such as large band gap bowing. Although there are various models to describe the conduction band of GaNAs, origin of the band gap bowing is still under debate. On the basis of perturbation theory, we show that the behavior of conduction band is mainly arising from intervalley mixing between Γ and L or X. By using renormalization technique and group theoretical treatment, we derive a reduced Hamiltonian which describes well the band gap shrinkage of GaNAs.

I. INTRODUCTION

III-V compound semiconductors containing nitrogen have been extensively studied for their properties different from those of conventional semiconductors.¹⁻⁷ In particular, behavior of conduction band edge of $\text{GaN}_x\text{As}_{1-x}$ (GaNAs) with small x attracts wide attention.⁸⁻¹⁰ As well known, the band gap of GaNAs decreases with nitrogen concentration. This is contrary to the conventional Vegard's law, that is, band gap of a mixed compound is well described as a linear interpolation of band gaps of constituent materials.

There have been various models to explain such behavior of GaNAs.¹¹⁻¹³ However, origin of the band gap bowing is still under debate. Band anticrossing model^{12,13} is widely used for phenomenological explanation of experimental results, however, its physical foundation is ambiguous. Band theories, which is a powerful tool to investigate electronic states, also have been applied to GaNAs. The tight-binding model,¹⁴⁻¹⁶ empirical pseudopotentials,¹⁷⁻²⁰ and the first principle calculations^{21,22} have been carried out to reproduce experimental results. Reliable results were obtained from these calculations, however, physical insight can be missed in handling the large matrix containing all the effects. In addition, when nitrogen concentration is very low, band calculations require much computational resources. As a result, calculations become difficult to carry out.

In this study, in order to investigate the conduction band of $\text{GaN}_x\text{As}_{1-x}$ with small x , we present a novel model derived from perturbation calculations using wavefunctions of bulk GaAs as bases. Investigation on behavior of conduction band has revealed that intervalley mixing induced by lattice distortion around nitrogen plays an important role for the band gap reduction of GaNAs. Utilizing this result, along with renormalization technique and symmetry considerations, we derive a simple equation to evaluate energy of the conduction band of GaNAs.

II. THEORY

A. Overview of band calculation procedure

First, we briefly review the procedure to calculate electronic states of bulk GaAs within the empirical pseudopotential

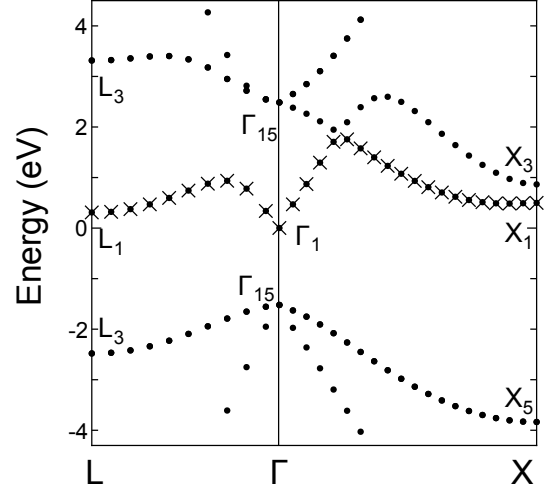


FIG. 1. Dispersion curves of bulk GaAs calculated by using plane wave bases and empirical pseudopotentials. The lowest conduction band, which we consider in this study, is denoted by crosses. Origin of energy axis is set to the conduction band edge.

method¹⁷ to be used as the basis in the following calculations.

Hamiltonian of bulk GaAs is given by a summation of kinetic energy and atomic potential energy $V(\mathbf{r})$ as

$$\mathcal{H}_0 = -\frac{\hbar^2 \nabla^2}{2m} + V(\mathbf{r}), \quad (1)$$

with

$$V(\mathbf{r}) = \sum_i [V_{\text{Ga}}(\mathbf{r} - \boldsymbol{\tau} - \mathbf{R}_i) + V_{\text{As}}(\mathbf{r} - \mathbf{R}_i)], \quad (2)$$

where V_{Ga} (V_{As}) is atomic pseudopotential of Ga (As) located in a unit cell specified by a lattice vector of the zinc blende structure \mathbf{R}_i . $\boldsymbol{\tau} = (a/4, a/4, a/4)$ with a the lattice constant is a vector which specifies position of Ga within a unit cell. Based on the empirical point of view, we regard that Coulomb interaction between electrons, exchange and correlation interactions, etc. are effectively included in the atomic pseudopotentials. We neglected the spin-orbit interaction. First, we calculate a Hamiltonian matrix

$$\mathcal{H}_0_{\mathbf{k}+\mathbf{G}_i, \mathbf{k}+\mathbf{G}_j} \equiv \langle \mathbf{k} + \mathbf{G}_i | \mathcal{H}_0 | \mathbf{k} + \mathbf{G}_j \rangle, \quad (3)$$

using plane wave basis functions

$$\langle \mathbf{r} | \mathbf{k} + \mathbf{G}_i \rangle = \frac{1}{\sqrt{\Omega}} e^{i(\mathbf{k} + \mathbf{G}_i) \cdot \mathbf{r}}, \quad (4)$$

with \mathbf{k} a wavevector, \mathbf{G}_i a reciprocal lattice vector, and Ω the system volume, respectively. By diagonalizing the Hamiltonian matrix, we can calculate a band energy

$$\varepsilon_{n,\mathbf{k}}^0 = \langle \psi_{n,\mathbf{k}}^0 | \mathcal{H}_0 | \psi_{n,\mathbf{k}'}^0 \rangle \delta_{\mathbf{k},\mathbf{k}'}, \quad (5)$$

and a wavefunction

$$\psi_{n,\mathbf{k}}^0(\mathbf{r}) = \sum_i c_{n,\mathbf{k} + \mathbf{G}_i} | \mathbf{k} + \mathbf{G}_i \rangle, \quad (6)$$

where $c_{n,\mathbf{k} + \mathbf{G}_i}$ is an eigenvector with an index n specifying band. The superscript “0” indicates non-perturbed quantities. In Figure 1, we show dispersion curves of bulk GaAs evaluated using empirical pseudopotential,¹⁷ where zero of the energy axis is set to the conduction band edge.

Using the bulk wavefunctions, we carry out perturbation calculations to evaluate energies of GaNAs. In what follows, we consider only the lowest conduction band plotted by crosses because we are interested in behavior of the conduction band edge labeled by Γ_1 in Fig. 1. From now on, we thus omit the index n which specifies band.

B. Perturbation matrix

Let us consider an $N \times N \times N$ supercell in which one of As atoms therein is replaced by a nitrogen atom. Although it is possible to apply the present theory for a system containing many nitrogen atoms, in this paper, we treat only the case of a single nitrogen atom. This supercell contains $4N^3$ primitive cells of the zinc blende structure.

Introduction of an N atom gives rise to change in crystalline potential. We take three factors into account: (i) change of the atomic potential from As to N, (ii) displacement of Ga atoms neighboring to the N atom, and (iii) displacement of As atoms at the second neighboring positions to the N atom. Then, the perturbation Hamiltonian is written as

$$\begin{aligned} \mathcal{H}'(\mathbf{r}) = & [V_N(\mathbf{r} - \mathbf{R}_I) - V_{As}(\mathbf{r} - \mathbf{R}_I)] \\ & + \sum_j [V_{Ga}(\mathbf{r} + \boldsymbol{\tau} - \mathbf{R}_j - \boldsymbol{\xi}_j) - V_{Ga}(\mathbf{r} + \boldsymbol{\tau} - \mathbf{R}_j)] \\ & + \sum_{j'} [V_{As}(\mathbf{r} - \mathbf{R}_{j'} - \boldsymbol{\eta}_{j'}) - V_{As}(\mathbf{r} - \mathbf{R}_{j'})], \end{aligned} \quad (7)$$

In the right hand side of eq. (7), the first term denotes potential change from that of As to N located at the position \mathbf{R}_I . The second and the third terms are arising from displacement of atoms neighboring to the nitrogen where $\boldsymbol{\xi}_j$ and $\boldsymbol{\eta}_{j'}$ are the displacement of the first neighboring Ga and the second neighboring As, respectively. The indices j and j' run through so that $\mathbf{R}_j - \boldsymbol{\tau} + \boldsymbol{\xi}_j$ and $\mathbf{R}_{j'} + \boldsymbol{\eta}_{j'}$ indicate the positions of the first neighboring four Ga atoms and the second neighboring twelve As atoms, respectively. We set $\boldsymbol{\xi}_j$ so that the Ga atoms

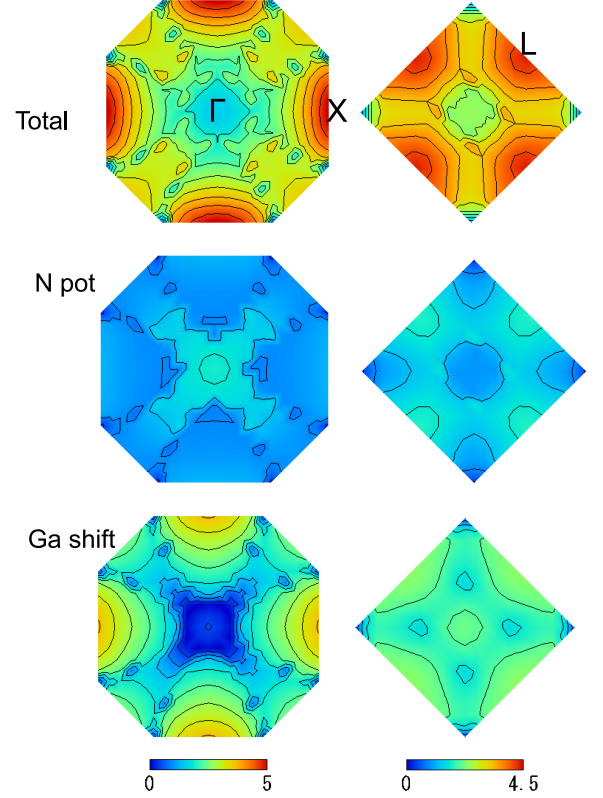


FIG. 2. (Color Online) Matrix element $|\mathcal{H}'_{k',k}|$ with $k' = (0,0,0)$ is plotted as a function of \mathbf{k} on the $k_z = 0$ plane (left column) and $k_z = \pi/a$ plane (right column) of the first Brillouin zone. From the top to bottom, total value of the matrix elements, contribution from the factor (i), and contribution from the factor (ii) are plotted in the unit of eV.

approach to the N atom by 0.38 \AA . Similarly, $\boldsymbol{\eta}_{j'}$ was determined so that the second neighboring As atoms approach to the N by 0.1 \AA . These values of atom displacements were determined from total energies evaluated by the first principle calculations using CASTEP package.

We calculated matrix elements of the perturbation Hamiltonian between the Bloch states of bulk GaAs taking the three factors (i), (ii), and (iii) mentioned above into account. In Fig. 2, we plot absolute value of the matrix elements

$$\mathcal{H}'_{k',k} \equiv \left(\frac{\Omega}{\Omega_{uc}} \right) \langle \psi_{k'}^0 | \mathcal{H}' | \psi_k^0 \rangle, \quad (8)$$

for $k' = \Gamma$ as a function of \mathbf{k} . $\Omega_{uc} = a^3/4$ is the zinc blende unit cell volume. On the left column, $|\mathcal{H}'_{\Gamma,k}|$ are plotted on the $k_z = 0$ plane which contains the Γ and X-points. On the right column, $|\mathcal{H}'_{\Gamma,k}|$ on the $k_z = \pi/a$ plane (the L-point is included) are shown. Note that different scales are used for figures in the left and right columns and that the values are in unit of eV. From top to bottom, total value, contribution from the factor (i), and contribution from the factor (ii) are plotted, respectively. We do not show contribution from the factor (iii) the position shift of second neighboring As, since this is much smaller than others. We note that the matrix elements are ba-

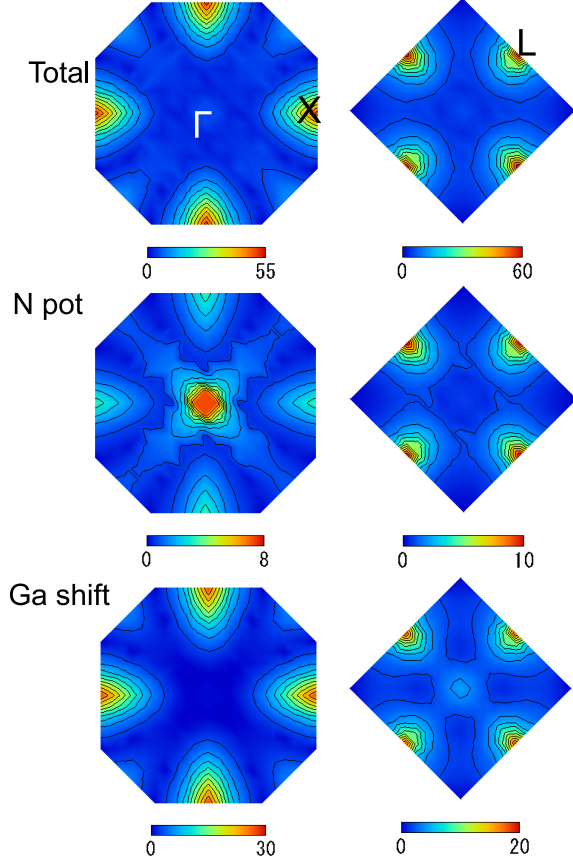


FIG. 3. (Color Online) $|\mathcal{H}'_{\Gamma,k}|^2/|\epsilon_{\Gamma}^0 - \epsilon_k^0|$ with $k' = (0, 0, 0)$ is plotted on the $k_z = 0$ plane (left column) and $k_z = \pi/a$ plane (right column) of the first Brillouin zone. From the top to bottom, total value, contribution from the factor (i), and contribution from the factor (ii) are plotted.

sically negative values, although we plot absolute values since they are complex quantities. We see that $|\mathcal{H}'_{\Gamma,k}|$ takes a large value when \mathbf{k} is X and L. We also see that the effect of displacement of neighboring Ga atoms is larger than that of the N potential.

Fig. 3 shows the quantity, $|\mathcal{H}'_{\Gamma,k}|^2/|\epsilon_{\Gamma}^0 - \epsilon_k^0|$ plotted as a function of \mathbf{k} . Similar to Fig. 2, total value, contribution from nitrogen potential, and displacement of Ga atoms are plotted from top to bottom. It is seen that $|\mathcal{H}'_{\Gamma,k}|^2/|\epsilon_{\Gamma}^0 - \epsilon_k^0|$ is largest when \mathbf{k} is the L-state, although the matrix element for the X-state is larger than that for the L-state. This is because energy difference between the L and Γ , $|\epsilon_{\Gamma}^0 - \epsilon_L^0|$, is smaller than $|\epsilon_{\Gamma}^0 - \epsilon_X^0|$. We also see that the N potential gives rise to mixing between the Γ -state and states in vicinity of Γ , whereas displacement of Ga atoms gives rise to the intervalley mixing. These results indicate that mixing between the Γ and L-states and/or between the Γ and X-states is relevant to the band gap reduction.

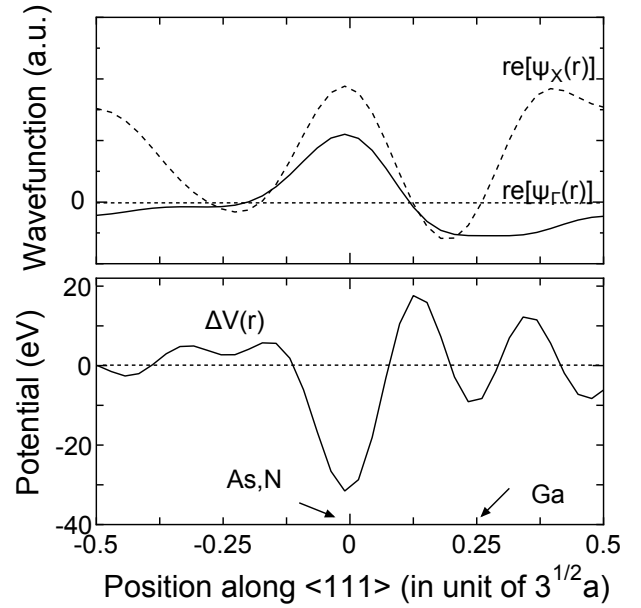


FIG. 4. Upper panel: wavefunctions of the Γ -state and X-state are plotted along the $\langle 111 \rangle$ direction by solid and dashed curves, respectively. Lower panel: Perturbation potential along the $\langle 111 \rangle$ direction is plotted by solid curve. The arrows show positions of As (N) and Ga. The horizontal dotted line shows zero.

C. Character of wavefunctions and matrix elements

We can discern the \mathbf{k} -dependence of the perturbation matrix elements from wavefunctions of bulk GaAs. In the upper panel of Fig. 4, the solid and dashed curves show $\psi_{\Gamma}^0(\mathbf{r})$ and $\psi_X^0(\mathbf{r})$ plotted along the $\langle 111 \rangle$ direction. The As (or N) atom locates at the position 0.0, and a Ga atom without displacement locates at +0.25 as indicated by arrows. It is seen that the Γ -state wavefunction consists of anti-bonding coupling between an s -like orbital of As and an s -like orbital of Ga. We also observe that the wavefunction around Ga is largely extended. The X-state consists of anti-bonding coupling between s -like orbital of As and p -like orbital of Ga which has a node at the Ga position. The L-state has character similar to the X-state though it is not shown in the figure.

In the lower panel, we plot perturbation potential along the $\langle 111 \rangle$ direction. We observe that the N atom gives rise to negative potential with s -like symmetry. On the other hand, perturbation potential around the Ga position is anti-symmetric around the Ga, that is, p -like symmetry.

These curves of crystalline potential and wavefunctions enable us to make qualitative interpretation on the matrix elements shown in the previous section. First, we consider the diagonal element $\mathcal{H}'_{\Gamma,\Gamma}$. This quantity is arising mainly from N potential because ψ_{Γ}^0 has a large amplitude at the N position. On the other hand, shift of Ga contributes little to $\mathcal{H}'_{\Gamma,\Gamma}$. This is because ψ_{Γ}^0 has s -like character around Ga. As we have noted, potential change due to Ga displacement is of p -character. Integration $|\psi_{\Gamma}^0|^2 \times \Delta V$ around the Ga atom will make the matrix element small. The coupling between Γ and L is also determined in the similar mechanism.

For the coupling between the Γ - and X-states $\mathcal{H}'_{\Gamma,X}$, shift of Ga atoms has an important role. From Fig. 4, we see that ψ_{Γ}^0 has s -like symmetry around the Ga atom, whereas both ψ_X^0 and \mathcal{H}' have p -like symmetry. Therefore, we anticipate that multiplication of these three quantities becomes even function around Ga, which enlarges the matrix element $\mathcal{H}'_{\Gamma,X}$.

We noted that contribution from shift of the second neighboring As atoms is small. This is also understood from symmetry. Although displacement of As atoms is about 1/3 of that of Ga atoms, contribution might be large because of larger number (12) of neighboring As atoms. As we have noted, atom's position change gives rise to perturbation potential with p -like symmetry. As seen from Fig. 4, both the Γ -state and X-state have s -like charge distribution around As atoms. From a simple consideration on symmetry, we see that $\langle \psi_{\mathbf{k}}^0 | \mathcal{H}' | \psi_{\mathbf{k}'}^0 \rangle$ with \mathbf{k} and \mathbf{k}' Γ or X has a small value.

These results indicates that mixing between Γ and X or between Γ and L induced by lattice distortion around N gives rise to band gap reduction of GaNAs.

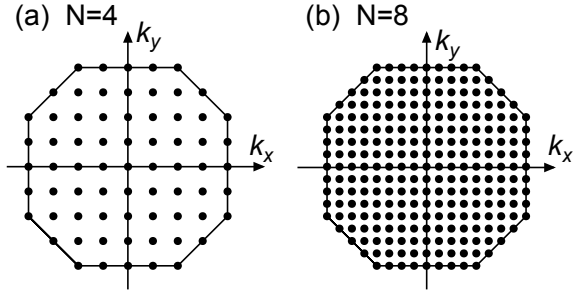


FIG. 5. Reciprocal lattice vectors used in perturbation calculations for (a) $4 \times 4 \times 4$ and (b) $8 \times 8 \times 8$ supercells. Note that equivalent points are excluded in the following calculations though they are plotted in the figures.

D. Band gap shrinkage

The matrix elements of the perturbation Hamiltonian for a single N atom in an $N \times N \times N$ supercell are written as

$$\mathcal{H}'_{\mathbf{k},\mathbf{k}'}^{(N)} = \frac{1}{4N^3} \langle \psi_{\mathbf{k}}^0 | \mathcal{H}' | \psi_{\mathbf{k}'}^0 \rangle, \quad (9)$$

where $1/4N^3$ is a factor to be normalized over the supercell. The states \mathbf{k} and \mathbf{k}' at which $\mathcal{H}'_{\mathbf{k},\mathbf{k}'}^{(N)}$ is evaluated are obtained as follows: Since the perturbation potential has translational symmetry with a period Na in all the x -, y -, and z -directions, $\langle \psi_{\mathbf{k}}^0 | \mathcal{H}' | \psi_{\mathbf{k}'}^0 \rangle$ must be unchanged when $\mathcal{H}'(\mathbf{r})$ is replaced by $\mathcal{H}'(\mathbf{r} + \mathbf{R})$ with a lattice vector of the supercell \mathbf{R} . From this, the wavevectors \mathbf{k} and \mathbf{k}' in eq. (9) must satisfy a relation

$$\mathbf{k} - \mathbf{k}' = \frac{2\pi}{Na} (n_x, n_y, n_z), \quad (10)$$

with n_x, n_y , and n_z integers. In Figs. 5 (a) and (b), the dots indicate possible $\mathbf{k}-\mathbf{k}'$ plotted on the first Brillouin zone of the zinc blende structure for $N = 4$ and $N = 8$, respectively. Note

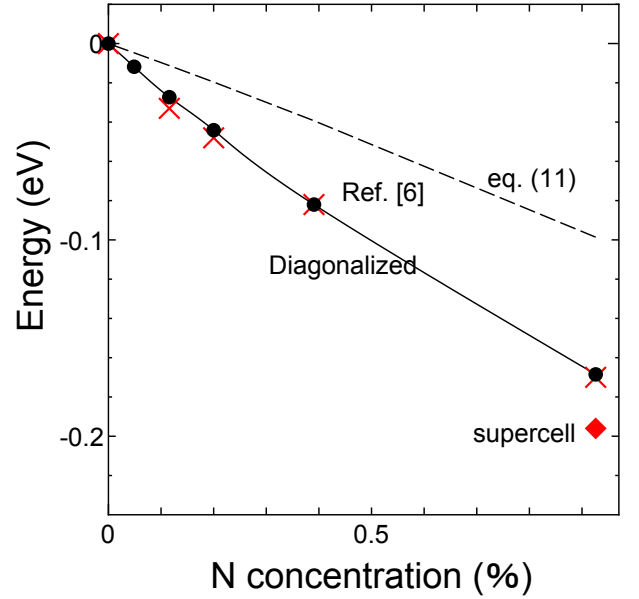


FIG. 6. (Color Online) Energies of conduction band edge are shown. Dashed curves show results of second order perturbation, evaluated by eq. (11). Filled circles show results calculated by diagonalizing full Hamiltonian matrix given by eq. (12). For comparison, theoretical data from Ref. [6] and results of supercell calculation are also plotted by cross and square, respectively.

that some points on the border are equivalent. For example, $2\pi/a(1, 0, 0)$ and $2\pi/a(-1, 0, 0)$ are identical and thus one of them must be excluded, though both are plotted in the figure. Excluding such equivalent points, we have $4N^3$ \mathbf{k} -points in the first Brillouin zone to be mixed due to the perturbation potential; there are 256 points for $N = 4$ and 2048 points for $N = 8$ necessary for calculations. We also note that these \mathbf{k} -points are the points that are folded onto the Γ -point in the Brillouin zone of the $N \times N \times N$ supercell. We can calculate conduction band energy from $\mathcal{H}'_{\mathbf{k},\mathbf{k}'}^{(N)}$ given by eq. (9) with bulk GaAs states shown in Fig. 5.

We may evaluate energy of the conduction band edge ε_{Γ} using the matrix elements by perturbation expansion. Up to the second order term, the energy change is given by

$$\varepsilon_{\Gamma} = \frac{1}{4N^3} \langle \psi_{\Gamma}^0 | \mathcal{H}' | \psi_{\Gamma}^0 \rangle + \frac{1}{(4N^3)^2} \sum_{\mathbf{k}} \frac{|\langle \psi_{\Gamma}^0 | \mathcal{H}' | \psi_{\mathbf{k}}^0 \rangle|^2}{\varepsilon_{\Gamma}^0 - \varepsilon_{\mathbf{k}}^0}, \quad (11)$$

where $x = 1/4N^3$ is nitrogen concentration. As we show in Fig. 6 by dashed curve, the second order perturbation is insufficient to explain experimental results, indicating that higher order perturbation energies are necessary since the potential change due to nitrogen is far from moderate.

Then, in order to evaluate energy of conduction band edge, we diagonalized a matrix

$$\mathcal{H}_{\mathbf{k},\mathbf{k}'}^{(N)} \equiv \langle \psi_{\mathbf{k}}^0 | \mathcal{H}_0 | \psi_{\mathbf{k}'}^0 \rangle + \mathcal{H}'_{\mathbf{k},\mathbf{k}'}^{(N)}. \quad (12)$$

Results are shown in Fig. 6 by filled circles. For comparison, we plot theoretical data from Ref. [6] by crosses. We also plot a result of supercell calculation with cutoff energy 3.0

Ryd. We see that the present perturbation calculations yield reasonable results.

III. REDUCED HAMILTONIAN

As we have shown in the previous section, proper energies were evaluated by diagonalizing a Hamiltonian matrix of $4N^3 \times 4N^3$ size. Mixing between the Γ -state and other \mathbf{k} -states due to nitrogen doping gives rise to the reduction of the conduction band edge. Among the states, the mixing between Γ and L is the largest. This fact leads us to an idea that we may have an effective Hamiltonian with only the Γ and L as bases. For this purpose, we applied Lödin's theory²³ described in detail in appendix A. In the present case where bases are the Γ and four L-states, we can reduce the size of the perturbation Hamiltonian down to 5×5 as shown in eqs. (A8) and (A9).

Further reduction of Hamiltonian is possible by applying group theoretical consideration. Since the four L-states are degenerated, any linear combinations among them satisfy the Schrödinger equation. This fact allows us to make a suitable combination that mixes (or does not mix) with the Γ -state. Coefficients for such a linear combination among the L-states are obtained considering symmetry of the L-state. Following standard procedure to obtain normal modes of an irreducible representation of the point group T_d , we symmetrize the linear combinations among the four L-states, $L_1 \sim L_4$.^{24,25} In this way, we have a singlet state

$$\psi_{\bar{L}} = \frac{1}{2}\psi_{L_1} + \frac{1}{2}\psi_{L_2} + \frac{1}{2}\psi_{L_3} + \frac{1}{2}\psi_{L_4}, \quad (13)$$

and triplet states

$$\begin{aligned} \psi_{L'} &= \frac{1}{\sqrt{2}}\psi_{L_2} - \frac{1}{\sqrt{2}}\psi_{L_3}, \\ \psi_{L''} &= -\frac{1}{\sqrt{2}}\psi_{L_1} + \frac{1}{\sqrt{2}}\psi_{L_4}, \\ \psi_{L'''} &= \frac{1}{2}\psi_{L_1} - \frac{1}{2}\psi_{L_2} - \frac{1}{2}\psi_{L_3} + \frac{1}{2}\psi_{L_4}. \end{aligned}$$

However, we have to note that these coefficients depend on situations such as nitrogen position, choice of origin, and trivial phase of wavefunctions etc. It is necessary to consider situations carefully in evaluating the coefficients.

Since the singlet state given by eq. 13 connects with the Γ -state and the triplet states do not, we can transform the 5×5 reduced matrix into a form

$$U^\dagger \tilde{\mathcal{H}}_{k,k'}^{(N)} U = \left[\begin{array}{cc|ccc} \tilde{\varepsilon}_\Gamma^0 & \tilde{V}_{\Gamma L} & 0 & 0 & 0 \\ \tilde{V}_{\Gamma L}^* & \tilde{\varepsilon}_L^0 - 3|\tilde{V}_{LL}| & 0 & 0 & 0 \\ \hline 0 & 0 & \tilde{\varepsilon}_L^0 + |\tilde{V}_{LL}| & 0 & 0 \\ 0 & 0 & 0 & \tilde{\varepsilon}_L^0 + |\tilde{V}_{LL}| & 0 \\ 0 & 0 & 0 & 0 & \tilde{\varepsilon}_L^0 + |\tilde{V}_{LL}| \end{array} \right], \quad (14)$$

with a matrix U in the form

$$U = \left[\begin{array}{c|cccc} 1 & 0 & 0 & 0 & 0 \\ \hline 0 & & & & \\ 0 & & & & \\ 0 & & & & \\ 0 & & & & \end{array} \right], \quad (15)$$

where 4×4 submatrix U_L is consisting of the coefficients of the linear combinations mentioned above. From this reduced matrix, we have energies of the Γ - and L-states as

$$\varepsilon_\Gamma = \frac{(\tilde{\varepsilon}_\Gamma^0 + \tilde{\varepsilon}_L^0 - 3|\tilde{V}_{LL}|) - \sqrt{(\tilde{\varepsilon}_\Gamma^0 - \tilde{\varepsilon}_L^0 + 3|\tilde{V}_{LL}|)^2 + |\tilde{V}_{\Gamma L}|^2}}{2}, \quad (16a)$$

$$\varepsilon_L^- = \frac{(\tilde{\varepsilon}_\Gamma^0 + \tilde{\varepsilon}_L^0 - 3|\tilde{V}_{LL}|) + \sqrt{(\tilde{\varepsilon}_\Gamma^0 - \tilde{\varepsilon}_L^0 + 3|\tilde{V}_{LL}|)^2 + |\tilde{V}_{\Gamma L}|^2}}{2}, \quad (16b)$$

$$\varepsilon_L^+ = \tilde{\varepsilon}_L^0 + |\tilde{V}_{LL}|. \quad (16c)$$

As seen in eqs. (A8) and (A9), the elements of the reduced matrix $\tilde{\varepsilon}_\Gamma^0$ etc. depend on E . We evaluated the elements as follows: In evaluating band edge energy ε_Γ , we set $E = \varepsilon_\Gamma^0$ and in evaluating L-point energy ε_L^\pm , we set $E = \varepsilon_L^0$.

In Fig. 7, we show energies calculated by the reduced Hamiltonian. ε_Γ and ε_L^\pm are plotted by squares and triangles, respectively. For comparison, we also plot the energies evaluated by diagonalization which were already shown in Fig. 6. For the Γ -state, the two methods give rise to almost the same results. This good agreement indicates validity of renormalization procedure.

As for the L-state energy, behavior of ε_L^- is similar to that of $E_0 + \Delta_0$ transition⁶. ε_L^+ seems corresponding to the E_+ transition.^{6,21,26} See, for example, Fig. 4 of Ref. [6]. However, further verification is necessary to apply the present theory to high energy states of GaNAs. In the present paper, we derived Γ L-reduced Hamiltonian, paying attention mainly to band gap reduction. However, many levels are observed in high energies in GaNAs,²⁶ and thus only Γ and L might be insufficient for description of high energy states. It is possible to construct Γ X- or Γ XL-reduced Hamiltonian in the same way. To investigate higher states, inclusion of the X-state would be necessary.

Band calculations using supercell can treat high energy states. For example, in Ref. [21] where the first principle calculations were carried out, the E_+ transition is assigned to transition to the L-state.²¹ In such calculations, however, we have a difficulty in picking up the state under attention, because of a number of states accumulated in energy due to multiply folded bands. In addition, as we have noted, some L(X)-states mix with the Γ -state and some do not, resulting in different dependence on N concentration. It is not straight forward to investigate high energy states by the supercell calculations. On the other hand, in the present theory, we can easily obtain high energy states.

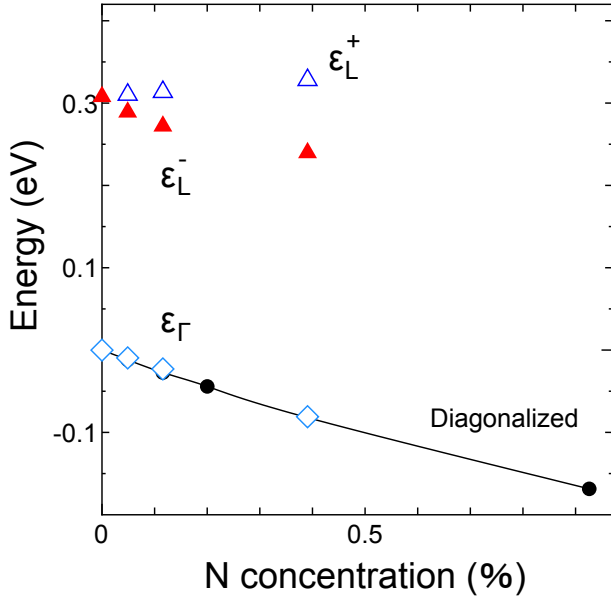


FIG. 7. (Color Online) Energies calculated by the reduced Γ -L Hamiltonian. ε_Γ , ε_L^- and ε_L^+ evaluated by eqs. (16a)–(16c) are plotted by square, filled triangle, and open triangle, respectively. Filled circles show energies evaluated by diagonalization of full Hamiltonian, which was already shown in Fig. 6.

In Fig. 8, we show elements of the reduced Hamiltonian. $\tilde{\varepsilon}_\Gamma^0$ and $\tilde{\varepsilon}_L^0 - 3|\tilde{V}_{\Gamma L}|$ are plotted in the upper panel and $\tilde{V}_{\Gamma L}$ is plotted in the lower panel as functions of nitrogen concentration. The squares show the values for $E = \varepsilon_\Gamma^0$ used to evaluate Γ -state energy, whereas triangles show the value with for $E = \varepsilon_L^0$ for L-state calculation. Present scheme where Γ - and L-states are retained as bases of the reduced Hamiltonian is inapplicable when N the supercell dimension is an odd number, because the L-point is not included in the set of \mathbf{k} -points necessary for perturbation calculation (see Fig. 5). Thus, calculations were carried out only for $N = 4, 6$ and 8 as shown by the squares and triangles in Fig. 7. Fortunately, as shown in Fig. 8, dependence of the matrix elements on nitrogen concentration is nearly linear, we can interpolate the matrix elements for calculating wide range of nitrogen concentrations.

IV. CONCLUSIONS

We presented a model to describe the conduction band of dilute nitride compound GaNAs. Using wavefunctions of conduction band of bulk GaAs as bases, we carried out perturbation calculations. Calculated perturbation matrix elements show that Γ -L mixing and/or Γ -X mixing are important for the band gap reduction. Though conventional second order formula yields a poor result, diagonalization of the full Hamiltonian matrix reveals that the present method brings about reasonable results. By remaining Γ - and L-states, we renormalized other states to derive effective 2×2 reduced Hamiltonian, which also describes well band gap reduction due to nitrogen.

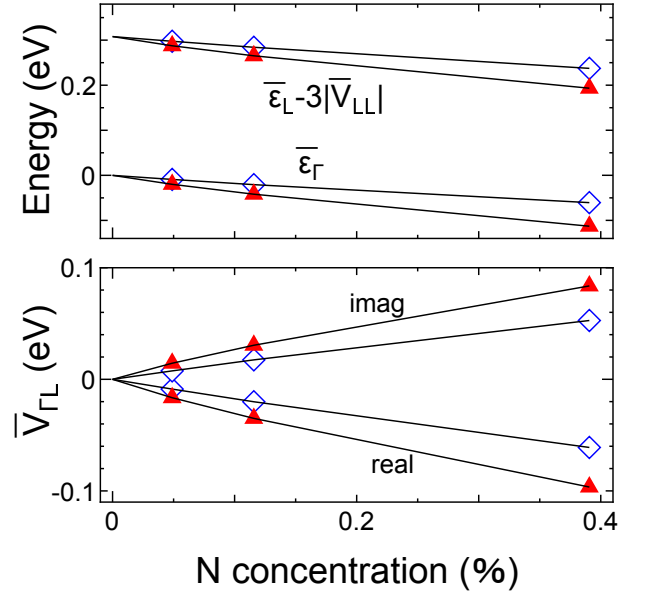


FIG. 8. (Color Online) Elements of reduced Hamiltonian are plotted as functions of nitrogen concentration. In the upper panel, ε_Γ^0 and ε_L^0 are plotted. In the lower panel, real and imaginary parts of $V_{\Gamma L}$ are plotted. Squares (triangles) are values to evaluate ε_Γ^0 (ε_L^0). Note that when nitrogen concentration is zero, these quantities take the values of bulk GaAs.

Appendix A: Renormalization procedure to reduce Hamiltonian

We show the procedure to reduce size of the Hamiltonian by renormalizing states whose interaction with the Γ -state is weak.²³ First, we divide basis functions into two groups: (A) states to be bases of the reduced Hamiltonian, and (B) the others. The states of the group (A) are those that interact with Γ strongly. By rearranging order of the bases, we rewrite the matrix $\mathcal{H}_{k,k'}^{(N)}$ in the form

$$\mathcal{H}_{k,k'}^{(N)} = \begin{bmatrix} \mathcal{H}_A & \mathcal{H}_{AB} \\ \mathcal{H}_{BA} & \mathcal{H}_B \end{bmatrix}, \quad (\text{A1})$$

where \mathcal{H}_A is a matrix consisting of the states belonging to the group (A), and so on. We omitted the indices \mathbf{k} , \mathbf{k}' and (N) in the right hand side for simplicity.

The secular equation is then written as

$$\begin{bmatrix} \mathcal{H}_A - E\mathbf{1} & \mathcal{H}_{AB} \\ \mathcal{H}_{BA} & \mathcal{H}_B - E\mathbf{1} \end{bmatrix} \begin{bmatrix} c_A \\ c_B \end{bmatrix} = \begin{bmatrix} 0 \\ 0 \end{bmatrix}, \quad (\text{A2})$$

where $\mathbf{1}$ is a unit matrix, 0 a zero vector, and c_A and c_B are column vectors with corresponding size. Owing to the choice of states for the groups (A) and (B), we expect that elements of the matrices \mathcal{H}_B , \mathcal{H}_{AB} and \mathcal{H}_{BA} are small, so that we can treat these quantities within lower order terms of expansion series.

Multiplying block by block, eq. (A2) is written as

$$(\mathcal{H}_A - E\mathbf{1})c_A + \mathcal{H}_{AB}c_B = 0, \quad (\text{A3})$$

and

$$\mathcal{H}_{BA} c_A + (\mathcal{H}_B^D - E\mathbf{1}) c_B + \mathcal{H}_B^O c_B = 0, \quad (\text{A4})$$

where \mathcal{H}_B^D and \mathcal{H}_B^O denote diagonal and off-diagonal parts of \mathcal{H}_B , respectively. We rewrite eq. (A4) in the form

$$c_B = (E\mathbf{1} - \mathcal{H}_B^D)^{-1} \mathcal{H}_{BA} c_A + (E\mathbf{1} - \mathcal{H}_B^D)^{-1} \mathcal{H}_B^O c_B. \quad (\text{A5})$$

This expression enables us to calculate c_B recursively. The lowest order expression for c_B is readily obtained by setting $c_B = 0$ in the right hand side. Setting $c_B = 0$ after replacing c_B in the right hand by the right hand side itself, we have the second expression to c_B as

$$c_B = (E\mathbf{1} - \mathcal{H}_B^D)^{-1} \mathcal{H}_{BA} c_A + (E\mathbf{1} - \mathcal{H}_B^D)^{-1} \mathcal{H}_B^O (E\mathbf{1} - \mathcal{H}_B^D)^{-1} \mathcal{H}_{BA} c_A. \quad (\text{A6})$$

In this way, we can express c_B in a series until suitable accuracy is obtained. Once we have c_B , by inserting the expression of c_B into eq. (A3), we have a secular equation

$$\left[\mathcal{H}_A + \mathcal{H}_{AB} (E\mathbf{1} - \mathcal{H}_B^D)^{-1} \mathcal{H}_{BA} + \mathcal{H}_{AB} (E\mathbf{1} - \mathcal{H}_B^D)^{-1} \mathcal{H}_B^O (E\mathbf{1} - \mathcal{H}_B^D)^{-1} \mathcal{H}_{BA} \cdots - E\mathbf{1} \right] c_A = 0. \quad (\text{A7})$$

Dimension of the matrices in this equation is that of the group (A). We thus have the reduced Hamiltonian

$$\tilde{\mathcal{H}}_{k,k'}^{(N)} = \mathcal{H}_A + \mathcal{H}_{AB} \left[g(E) + g(E) \mathcal{H}_B^O g(E) + g(E) \mathcal{H}_B^O g(E) \mathcal{H}_B^O g(E) \cdots \right] \mathcal{H}_{BA}, \quad (\text{A8})$$

with

$$g(E) = (E\mathbf{1} - \mathcal{H}_B^D)^{-1}, \quad (\text{A9})$$

in which effects from states of group (B) are effectively contained.

-
- ¹ M. Kondow, K. Uomi and T. Nozue, Jpn. J. Appl. Phys. **33**, L1056 (1994).
² M. Weyers, M. Sato and H. Ando, Jpn. J. Appl. Phys. **31**, L853 (1992).
³ W. G. Bi and C. W. Tu, Appl. Phys. Lett. **70**, 1608 (1997).
⁴ C. Skierbiszewski, S. P. Lepkowski, P. Perlin, T. Suski, W. Jantsch, and J. Geisz, Physica E **13** 1078 (2002).
⁵ W. Shan, W. Walukiewicz, K. M. Yu, and J. W. Ager III, E. E. Haller, J. F. Geisz, D. J. Friedman, J. M. Olson, and Sarah R. Kurtz, and C. Nauka, Phys. Rev. B **62**, 4211 (2000).
⁶ P. H. Tan, X. D. Luo, Z. Y. Xu, Y. Zhang, A. Mascarenhas, H. P. Xin, C. W. Tu, and W. K. Ge, Phys. Rev. B **73**, 205205 (2006).
⁷ K. Uesugi, N. Morooka, and I. Suemune, Appl. Phys. Lett. **74**, 1254 (1999).
⁸ S. Noguchi, S. Yagi, D. Sato, Y. Hijikata, K. Onabe, S. Kuboya, and H. Yaguchi, IEEE J. Photovoltaics, **3**, 1287 (2013).
⁹ K. Sumiya, M. Morifuji, Y. Oshima, and F. Ishikawa, Applied Physics Express **6** 041002 (2013).
¹⁰ T. Fukushima, Y. Hijikata, H. Yaguchi, S. Yoshida, M. Okano, M. Yoshita, H. Akiyama, S. Kuboya, R. Katayama, K. Onabe, Physica E **42**, 2529 (2010).
¹¹ Chuan-Zhen Zhao, Na-Na Li, Tong Wei, Chun-Xiao Tang, and Ke-Qing Lu, Appl. Phys. Lett. **100**, 142112 (2012).
¹² W. Shan, W. Walukiewicz, J. W. Ager III, E. E. Haller, J. F. Geisz, D. J. Friedman, J. M. Olson, and S. R. Kurtz, Phys. Rev. Lett. **82**, 1221 (1999).
¹³ J. Wu, W. Walukiewicz, K. M. Yu, J. W. Ager III, E. E. Haller, Y. G. Hong, H. P. Xin, and C. W. Tu, Phys. Rev. B **65**, 241303 (2002).
¹⁴ A. Lindsay and E. P. O'Reilly, Phys. Rev. Lett. **93** 196402 (2004).
¹⁵ E. P. O'Reilly, A. Lindsay, S. Tomić and M. Kamal-Saadi, Semicond. Sci. Technol. **17** 870 (2002).
¹⁶ W. J. Fan, M. F. Li, and T. C. Chong, J. B. Xia, J. Appl. Phys. **79** 188 (1996).
¹⁷ L. Bellaiche, S.-H. Wei, and A. Zunger, Appl. Phys. Lett. **70** (1997).
¹⁸ L. Bellaiche, S.-H. Wei, and A. Zunger Phys. Rev. B **54**, 17568 (1996).
¹⁹ Kurt A. Mader and A. Zunger, Phys. Rev. B **50**, 17393 (1994).
²⁰ P. R. C. Kent and A. Zunger Phys. Rev. B, **64**, 115208 (2001)
²¹ V. Timoshevskii, M. Côté, G. Gilbert, and R. Leonelli, S. Turcotte, J.-N. Beaudry, P. Desjardins, S. Larouche, L. Martinu, and R. A. Masut, Phys. Rev. B **74**, 165120 (2006).
²² C. -K. Tan, J. Zhang, X. -H. Li, G. Liu, B. O. Tayo, and N. Tansu, J. Display Technol., **9**, 272L (2013).
²³ Pre-Olov Lödin, J. Chem. Phys. **19**, 1396 (1951).
²⁴ G. Burns, *Introduction to group theory with applications*, Academic Press, INC, New York 1977.
²⁵ H. Jones, *The theory of Brillouin zones and electronic states in crystals*, Second, revised edition, North-Holland, Amsterdam 1977.
²⁶ S. Francoeur, M. J. Seong, M. C. Hanna, J. F. Geisz, A. Mascarenhas, H. P. Xin, and C. W. Tu, Phys. Rev. B **68**, 075207 (2003).